RSC Advances

ROYAL SOCIETY OF CHEMISTRY

www.rsc.org/advances

Journal Name

RSCPublishing

ARTICLE

High-performance recyclable V-N-C catalysts for the direct hydroxylation of benzene to phenol using molecular oxygen

Cite this: DOI: 10.1039/xoxxoooooox

Received ooth January 2012,
Accepted ooth January 2012

DOI: 10.1039/xoxxoooooox

www.rsc.org/

Sensen. Shang,[ab] Bo Chen,[ab] Lianyue Wang,[a] Wen Dai,[a] Yi Zhang[a] and Shuang Gao*[a]

In this report, high-performance recyclable V-N-C catalysts for the direct hydroxylation of benzene to phenol using molecular oxygen were designed and prepared. Up to 12.6% yield of phenol with the selectivity as high as 97.8% was achieved employing V-N-C-*600* catalyst in acetonitrile. The catalytic recycling tests demonstrated that V-N-C-*600* catalyst exhibited high potential for reusability. The catalysts were characterized systematically by thermogravimetric analysis, fourier transform infrared spectroscopy, N_2 adsorption-desorption, powder X-ray diffraction, Raman spectra, X-ray photoelectron spectroscopy techniques and scanning electron microscope. It was considered that the interaction between surface nitrogen of supports and reactive vanadium species played an important role in the excellent stability in recycling of the heterogeneous V-N-C catalysts.

1. Introduction

Phenol is a crucial bulk commodity chemical in industry, which is widely used in the manufacturing of phenol resins, caprolactam, adipic acid, fibers, and many other chemicals.[1-3] Nowadays, more than 90% of the phenol is still being produced industrially by the three-step cumene process,[4] which involves unexpected high energy consumption and significant formation of side products such as acetone and methylstyrene. Therefore, the direct hydroxylation of benzene to phenol is potentially an area of great interest and still regarded as one of the 10 most difficult challenges in catalysis,[5] as the phenol selectivity is limited due to the higher oxidation reactivity of phenol when compared to benzene.[6] Indeed, endeavors have been made using green oxidants, such as O_2,[7-10] H_2O_2[11-18] or N_2O[19-23]. As for N_2O, despite its high selectivity to phenol, the main restriction for the wide application of N_2O is its complex operation process.[17] On the other hand, H_2O_2 is too expensive to be applied in commercial production. In this regard, it is highly desirable to develop an efficient catalytic system for the direct hydroxylation of benzene to phenol using O_2 as green and economical oxidant agent.[24]

In the past several decades, various catalytic systems, such as membrane process, high-temperature gas-phase and low-temperature liquid-phase catalytic reactions have been developed for this aerobic oxidation. After Mizukami *et al*. reported the direct hydroxylation of benzene to phenol in gas phase with molecular oxygen activated by dissociated hydrogen obtained from a palladium membrane at 2002,[24] Zhang *et al*. have been devoted to overcoming the instability of Pd membrane.[25, 26] Meanwhile, the utilization of noble metals largely increased the cost of the catalytic system. In addition, both the vast energy consumption and the unexpected hazard were caused by high-temperature gas-phase catalytic system. Consequently, developing low-temperature liquid-phase oxidation of benzene to phenol catalyzed by highly efficient non-noble metal catalysts, mainly containing Cu or V species, is drawing more and more attention from an economic and environmental point of view. Ohtani *et al*. tested a series of zeolites loaded with Cu as catalysts with molecular oxygen under atmospheric pressure at room temperature, giving a phenol yield of 1.69% with Cu-NaY as the best catalyst and ascorbic acid as a reducing agent at 1995.[27] After then, the Cu ion-exchanged HPMCM-41 catalysts were proved to be more active than the corresponding Cu catalysts supported on SiO_2, TiO_2, MgO, or NaY, even though with less than the phenol yield of 2%.[28] It was worth mentioning that the accumulation of H_2O_2 was confirmed during the liquid-phase oxidation process. Moreover, the yield of phenol over CuO-Al_2O_3 and Cu/Al_2O_3 catalysts prepared by Tsuruya *et al*. in different methods in the similar catalytic system were 1.25% and 2.5%, respectively.[29] Furthermore, in 2006 Gao *et al*. realized the direct hydroxylation of benzene to phenol by prereducing V/Al_2O_3 by ascorbic acid before reaction, even though only giving the phenol yield of 4.3%.[30] It was found that the V^{4+} valence

vanadium (VO^{2+}) was effective for the reaction. In addition, the V-containing polyoxometalates (POMs) of structure and property diversity were a group of widely studied catalysts in the hydroxylation process.[9, 31-34] To date, the highest phenol yield of more than 20% could be achieved by the synergy between copper and vanadium oxide species on the support SBA-15.[35] Most recently, Han *et al*. prepared VxOy@C catalysts derived from sucrose and NH_4VO_3 by hydrothermal method.[36] The catalysts showed good catalytic performance for the title reaction using oxygen as oxidant with a phenol yield of 12.2%. Unfortunately, supported vanadium catalysts for oxidation usually suffered from vast leaching of vanadium, which resulting in that the catalysts could not be recycled. Therefore, design and preparation of highly efficient recyclable catalysts for the direct hydroxylation of benzene to phenol still needed further investigation.

As it was reported that N-dopants in the carbon material could strengthen the interaction between the reactive species and supports,[37, 38] the introduction of N may contribute to overcome the leaching of reactive species. Bearing extreme chemical and thermal stability and easy accessibility of polyaniline (PANI)[39] in mind, we selected it as nitrogen and carbon precursor and $VO(acac)_2$ as metal precursor to realize facile one-pot synthesis of vanadium-supported N-doped carbon materials (designated as V-N-C). The use of such a polymer PANI as a nitrogen and carbon precursor promised a more uniform distribution of nitrogen sites on the surface, further resulted in a more uniform distribution of reactive vanadium species. The catalysts were characterized systematically using thermogravimetric analysis (TGA), fourier transform infrared spectroscopy (FTIR), N_2 adsorption-desorption, powder X-ray diffraction (XRD), Raman spectra, X-ray photoelectron spectroscopy techniques (XPS) and scanning electron microscope (SEM). Based on the above characterization, it was found that the special structure of V-N-C catalysts prepared at different pyrolysis temperature varied greatly as well as the chemical state, resulting in different catalytic performance on the direct hydroxylation of benzene to phenol with molecular oxygen as oxidant. Up to 12.6% yield of phenol was achieved with the selectivity as high as 97.8% employing V-N-C-*600* catalyst. The influence of reaction conditions, such as reaction time, reaction temperature, and oxygen pressure was investigated. Noteworthily, V-N-C-*600* catalyst could be recycled at least six times without significant decline of phenol yield. It was considered that the interaction between surface nitrogen of supports and reactive vanadium species played an important role in the good stability in recycling of the heterogeneous V-N-C catalysts.

2. Results and discussion

2.1 Structure characterization of V-N-C catalysts

The dynamic thermogravimetry analysis (TGA) and the corresponding differential thermogravitry (DTG) curves during the heat treatment of PANI-V composites were illustrated in Fig. 1. The DTG indicated a multi-stage pyrolysis. At least three features could be distinguished on the DTG curve. One feature appeared as a peak at around 100°C related to water desorption, if the material was not sufficiently dry. The most important feature was pointed out as a peak in a range of 200 to 400 °C. The highest mass change took place on the DTG trace and could be attributed to the decomposition of the remained acetate ligand. It also meant that the formation of VOx occurred. While the TG and DTG traces up to 500 °C showed no significant change of the PANI-V composites, it could be addressed to the reconstruction and carbonization of carbon nitride matrix PANI to form the N-doped graphene layers.

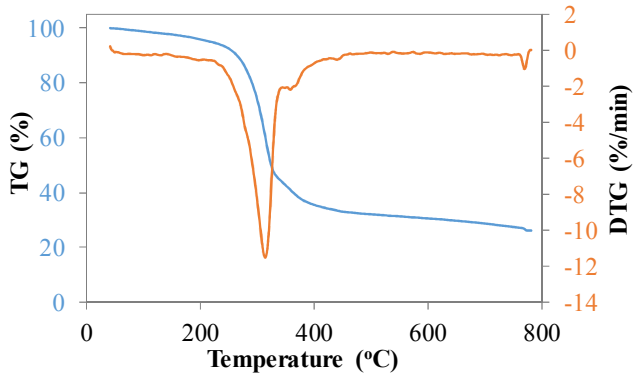

Fig. 1 The dynamic TG and the corresponding DTG curves during the heat treatment of PANI-V composites

Fourier transform infrared (FTIR) spectra of unpyrolyzed PANI-V composites and V-N-C catalysts (Fig. 2) showed that the benzene-type (1170 cm^{-1}) and quinone-type (1400 cm^{-1}) structures[40] on the main PANI chain transformed to other structures containing C=N (1630 cm^{-1}). The weak absorption bands at ca. 1020, 825, and 602 cm^{-1} of V-N-C catalysts were attributed to the stretching vibrations of isolated V=O groups[41] and the deformation modes of V-O-V chains[42]. Moreover, Fig. S1 illustrated the shape of N_2 adsorption-desorption isotherms of V-N-C-*600*, showing the presence of a certain degree of microporous structure. The textual parameters, including surface areas and pore volumes of V-N-C catalysts were summarized in Table S1. Increasing the pyrolysis temperature resulted in significant increase in the surface area and pore volume. Meanwhile, the pore size distributions of V-N-C catalysts were relatively broad.

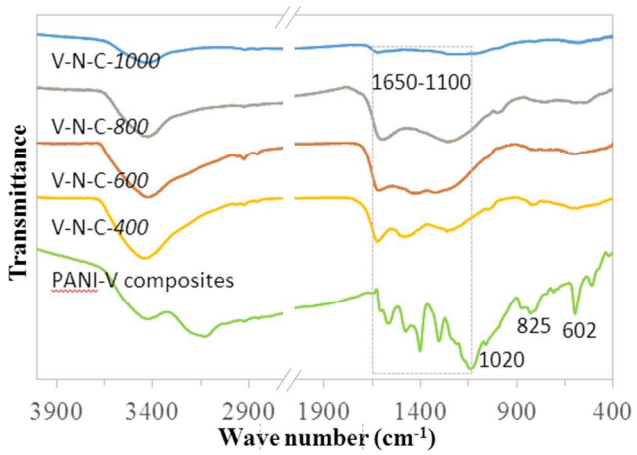

Fig. 2 FT-IR spectra of PANI-V composites and V-N-C catalysts.

The X-ray diffraction (XRD) patterns shown in Fig. 3 displayed the structures of V-N-C catalysts prepared at different temperatures. The broadened peak centers at 25 ° was observed, corresponding to the (002) plane of carbon material with low graphitization degree.[43] By contrast, this characteristic peak exhibited in XRD patterns of V-N-C-*600* catalyst was comparatively narrower than that in others, indicating pyrolysis treatment at 600 °C may lead to the formation of more ordered graphite carbon. In addition, the characteristic diffraction peaks of crystalline V_2O_3 were clearly found in the XRD patterns of V-N-C-1000 catalyst, though with very low crystallinity, which may be attributed to the high-temperature pyrolysis resulting in the formation of crystal phase V_2O_3. Moreover, Fig. S2 compared Raman spectra of V-N-C catalysts synthesized at different temperatures. As the highly ordered graphite shows a very weak D-band,[44] the low ratio of the D-band to G-band integrated intensities proved the formation of more and more ordered graphite structure during the heat treatment at 400, 600 °C, which was consistent with the result of XRD tests.

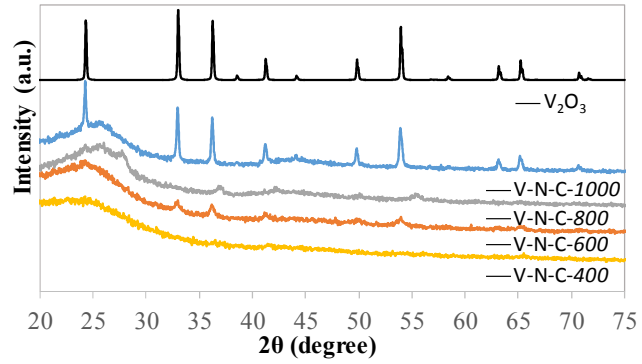

Fig. 3 XRD patterns of crystallite V_2O_3 and V-N-C catalysts.

X-ray photoelectron spectroscopy (XPS) measurements were conducted to elucidate the surface chemical composition of V-N-C catalysts. Fig. 4 demonstrated that the chemical composition of V-N-C catalysts was significantly different. As shown in Fig. 4e, it was clear that the increase in the pyrolysis temperature led to a sudden drop in nitrogen content, from 13.24 at.% to 2.95 at.%. This may be attributed to the breaking of the nitrogen-carbon bond.

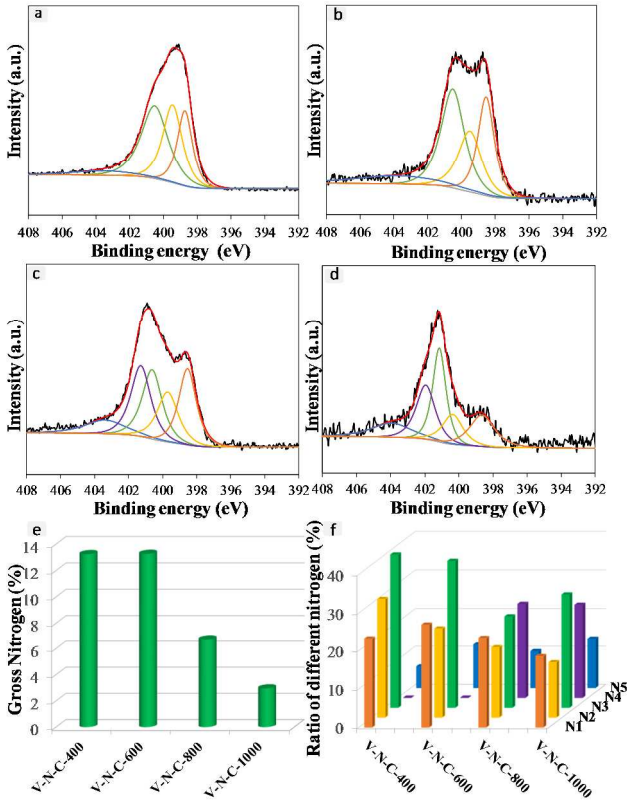

Fig. 4 XPS spectra of N 1s (a) V-N-C-*400*, (b) V-N-C-*600*, (c) V-N-C-*800*, (d) V-N-C-*1000*, (e) gross nitrogen-content of different catalysts, (f) Nitrogen configurations for different catalysts.

Nitrogen could be present in different forms of nitrogen doped carbon including pyridinic-N, pyrrolic-N, graphitic-N, quaternary-N, and pyridine-N-oxide. Fig. 4a-d showed the deconvoluted XPS spectra of N 1s of V-N-C catalysts. Meanwhile, three different signals having binding energies of 398.7 eV±0.2, 399.8 eV±0.2, and 401.0 eV±0.2, corresponded to pyridinic N, pyrrolic N, and graphitic N, respectively.[45, 46] The peak at the binding energy of 398.7 eV±0.2, N1, should also include a contribution from nitrogen bound to the metal (N−V), due to the small difference between binding energies of N−Metal and pyridinic N.[46, 47] Pyridinic N (probably including N−V) and graphitic N are generally believed to participate in the activation of molecular oxygen.[46-48] The N1 content increased to the maximum as the pyrolysis temperature increased from 400 to 600 °C, and then immediately began to gradually decrease with the continue increasing in the pyrolysis temperature (Fig. 4f). The pyrrolic-N (399.8 eV±0.2, N2) refers to the N atoms bonded with two carbon atoms, which is incorporated into five member heterocyclic rings. The N2 content quickly decreased as the pyrolysis temperature increased, which indicated that the N1 was more stable than the N2. As we know, quaternary-N (401.0 eV, N3) is the graphitic nitrogen in the centre of the heterocyclic rings, which is located in the perfect graphite plane by bonding with three carbon

atoms. However, for the peak at 401.9 eV±0.2, N4, some researchers believed that it was contributed to the pyridine-N-oxide[49] and some thought it reflected the presence of graphitic-N at the valley, which is located at the edge of the heterocyclic rings.[39, 50, 51] It had been reported that the nitrogen oxide functionalities exhibited low thermal stability.[49] Indeed, the ratio of N4 increased with the increase in the pyrolysis temperature. Therefore, this peak in this article should be assigned to graphite nitrogen, which was in agreement with the observations of Sharifi et al.[51] Insterestingly, the perfect graphite N3 ratio sharply decreased with the increase to 800 °C in the pyrolysis temperature, which mainly attributed to the sudden increase of the N4 ratio. It indicated that the structure of perfect graphite nitrogen-doped carbon structure transformed into other forms. Moreover, pyridine-N-oxide (403.5±0.2 eV, N5) refers to N atom bonded with two carbon atoms and one oxygen atom. The N5 content fluctuated in some degree as the temperature increased.

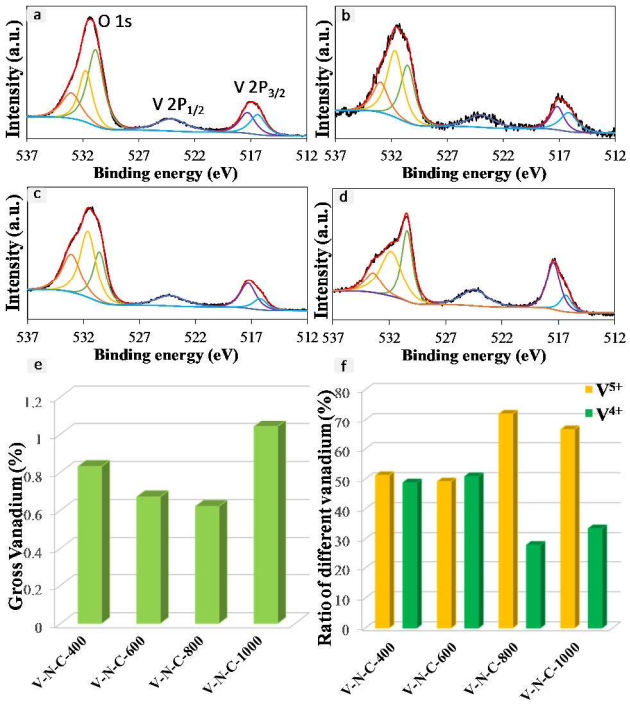

Fig. 5 XPS spectra of O 1s, V 2P (a) V-N-C-*400*, (b) V-N-C-*600*, (c) V-N-C-*800*, (d) V-N-C-*1000*, (e) gross vanadium-content of different catalysts, (f) Vanadium configurations for different catalysts.

From the XPS data, the O 1s profile could be separated into three peaks (Fig. 5). That was, there existed three types of O species, carbonyl groups, alcohol and/or ether groups, and carboxyl and/or ester groups at 531.6, 532.5 and 533.5 eV, respectively.[52] The XPS spectra of V-N-C catalysts showed the binding energy of V $2P_{1/2}$ at 523.4 eV and the binding energy of V $2P_{3/2}$ in the range of 515.5-517.0 eV,[30, 53] indicating the existence of V^{4+} and V^{5+} on the surface of different catalysts, but no V^{3+} (515.1eV). It was because the surface V^{3+} is easily oxidized to V^{4+} when exposed to air. Additionally, low content and amorphous phase of V^{4+} and V^{5+} resulted in that no corresponding diffraction peaks existed in the XRD patterns of V-N-C catalysts. Furthermore, Fig. 5e showed that the surface V contents of V-N-C catalysts were 0.83, 0.67, 0.62 and 1.04 wt% for V-N-C-*400*, V-N-C-*600*, V-N-C-*800* and V-N-C-*1000* catalysts, respectively. As shown in Fig. 5f, the ratio of surface V^{4+} of V-N-C-*600* catalyst was comparatively higher, while that of V-N-C-*1000* with the highest surface gross vanadium was lowest among them. The surface morphology of V-N-C-*600* catalyst was determined by SEM (Fig. S3). Furthermore, the VOx particles were uniformly incorporated in the nitrogen-doped carbon supports as shown in Fig. S4a-b. Moreover, as illustrated by energy-dispersive X-ray spectroscopy (EDXS) analysis (Fig. S4c), the particles contained vanadium.

2.2 Catalytic performances of V-N-C catalysts for the direct hydroxylation of benzene to phenol

A series of V-N-C catalysts were prepared by pyrolyzing PANI-V composites under different temperature. ICP tests indicated that V content in the catalysts increased gradually with the increase of the pyrolysis temperature, which may due to high temperature treatment resulted in a certain amount of loss of carbon nitride supports. Furthermore, the catalytic performances of V-N-C catalysts for the direct hydroxylation of benzene to phenol with molecular oxygen were evaluated. In all reactions, phenol and hydroquinone were produced without observing the formation of catechol and benzoquinone. As shown in Table 1, trace phenol was obtained in the absence of catalyst (Table 1, entry 1). Ascorbic acid was used as the sacrificial reductant, which proved to be essential for the hydroxylation reaction (Table 1, entry 2). To our delight, the yield of phenol first increased with pyrolysis temperature and then decreased with a threshold of 600°C, giving 11.8% yield with 97.0% selectivity. (Table 1, entry 3-6). Though not significant rangeability which may result from the inert reactivity of benzene, it was understandable considering that V-N-C-*600* catalyst with a higher ratio of surface V^{4+} active species performed better than others. On the contrary, V-N-C-*1000* catalyst with a lower ratio of surface V^{4+} only obtained 9.2% yield with 95.6% selectivity, even though the surface gross vanadium was higher than others (Table 1, entry 6), which was consistent with that V^{4+} have been proved to be more active for activating oxygen.[36, 54] In addition, it could be speculated that specific surface area and specific volume of catalysts are not the only factor affecting the catalytic performance in consideration of the highest specific surface area and specific volume of V-N-C-*1000* catalyst. Moreover, only trace phenol was obtained when N-C-*600* catalyst was used as catalyst, which proved that V species were necessary for the direct hydroxylation of benzene to phenol with molecular oxygen as oxidant (Table 1, entry 7). Next we studied the influence of reaction time on the direct hydroxylation of benzene to phenol over V-N-C-*600* catalyst. When the reaction time reduced to 6h, only 7.0% yield of phenol was obtained with 99.5% selectivity (Table 1, entry 8). When the reaction time was 12h, 9.6% yield of phenol was produced with up to 99.9% selectivity (Table 1, entry 9). When

the reaction time was further prolonged to 36h, the yield of phenol was increased to 12.6% with the selectivity slightly decreased to 97.8% (Table 1, entry 10), which was higher than that reported in the literature with acetonitrile as solvent and molecular oxygen as oxidant.[33, 36]

Table 1. The catalytic performance of V-N-C catalysts.

Entry	Catalyst[a]	V% (ICP)	Yield (%)[b]	Sel. (%)[b]
1[c]	None	0	Trace	--[d]
2[e]	V-N-C-*600*	4	Trace	--
3	V-N-C-*400*	4.3	10.1	98.7
4	V-N-C-*600*	4.0	11.8	97.0
5	V-N-C-*800*	6.4	10.8	97.0
6	V-N-C-*1000*	9.5	9.2	95.6
7	N-C-*600*	0	Trace	--
8[f]	V-N-C-*600*	4.0	7.0	99.5
9[g]	V-N-C-*600*	4.0	9.6	99.9
10[h]	V-N-C-*600*	4.0	12.6	97.8

[a] Reaction conditions: 10 mmol benzene, 1.4 mol% V, 0.88 g ascorbic acid, 2 g acetonitrile, 2 MPa O_2, 80 °C, 24 h. [b] Determined by GC. [c] Without an addition of catalysts. [d] No by-product was detected. [e] Without ascorbic acid. [f] 6 h. [g] 12 h. [h] 36 h.

Fig. 6 depicted the influence of reaction temperature on the direct hydroxylation of benzene to phenol over V-N-C-*600* catalyst. The yield of phenol first increased as the reaction temperature increased to 80 °C and then decreased. The decrease of the oxygen solubility with an increase of temperature was one of the main reasons for this phenomenon.[55] the self-oxidation of ascorbic acid as the sacrificial reductant prolonged the reaction,[29] which also caused the decline in the yield of phenol. Additionally, It was found when the reaction temperature was higher than 80 °C, the selectivity of phenol sharply decreased, indicating that overoxidation of benzene prefers higher reaction temperature.

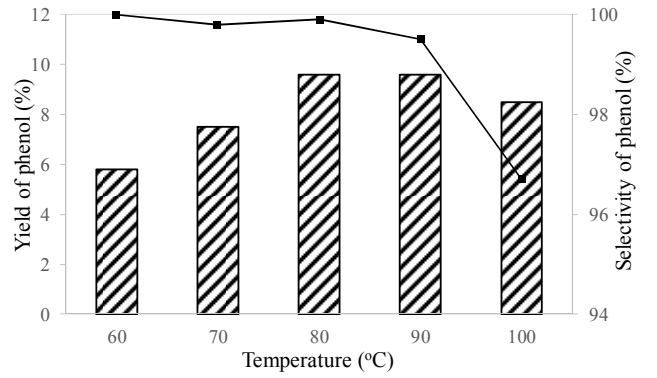

Fig. 6 The influence of reaction temperature on the direct hydroxylation of benzene to phenol over V-N-C-*600* catalyst. The yield (column) and selectivity (■) of phenol. Reaction conditions: 10 mmol benzene, 1.4 mol% V, 0.88 g ascorbic acid, 2g acetonitrile, 2 MPa O_2, 12 h.

The influence of oxygen pressure was also investigated (Fig. 7). In the low pressure range, the yield of phenol was enhanced to a maximum 10.7 % with the oxygen pressure increased to 3.0 MPa, which may be attributed to the larger solubility of oxygen at the higher oxygen pressure.[55] However, the selectivity of phenol significantly decreased at the same time. Especially, when the oxygen pressure further increased, the selectivity and yield of phenol were both obviously decreased. It was believed that too much oxygen might cause the overoxidation of phenol, which resulted in a decrease in the selectivity and yield of phenol.

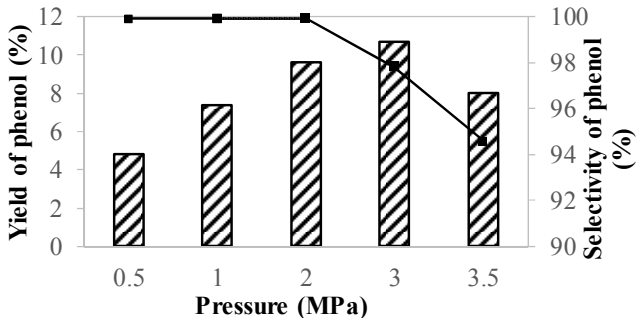

Fig. 7 The influence of oxygen pressure on the direct hydroxylation of benzene to phenol over V-N-C-*600* catalyst. The yield (column) and selectivity (■) of phenol. Reaction conditions: 10 mmol benzene, 1.4 mol% V, 0.88 g ascorbic acid, 2 g acetonitrile, 80 °C, 12 h.

The efficacy of a heterogeneous catalyst should also be evaluated from its recyclability and stability. V-N-C-*600* catalyst presented considerable recyclability towards the phenol formation with the above 98% selectivity over six catalytic cycles, as shown in Fig.8. The yield of phenol decreased during the first running cycle, while it obviously improved by calcining the recycled catalyst under flowing nitrogen at 400°C for 2 hours. It could be speculated that one possible reason accounting for the phenomenon was the absorption of substrate, product and high-boiling byproduct for the catalyst. Afterwards, the recycled catalyst presented nice recyclability, but a slight decrease compared with the first test, which may be due to the leaching of unstable V species (leaching of V after the first run: 17.9%, determined by ICP). Moreover, compared with fresh V-N-C-*600* catalyst, the FTIR spectra, XRD patterns and V XPS spectra of the reactivated catalyst after sixth run did not show any obvious change, as shown in Fig. S5 and S6. Considerable recyclability of V-N-C-*600* catalyst could be ascribed to the presence of the interaction of nitrogen and vanadium, which avoided the vast leaching of V, generally existing in the supported vanadium catalytic oxidation.

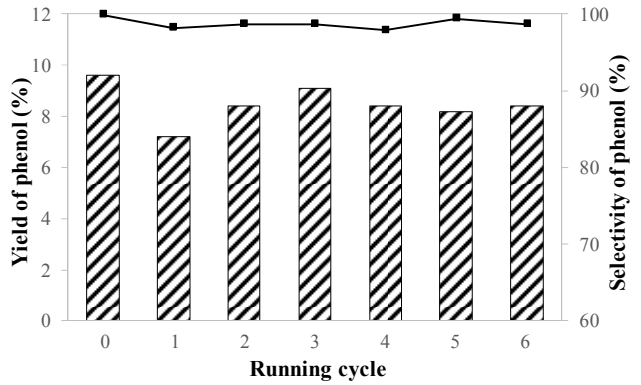

Fig. 8 Reuse of the catalysts for the direct hydroxylation of benzene to phenol. The yield (column) and selectivity (■) of phenol. Reaction conditions: 10 mmol benzene, 1.4 mol% V, 0.88 g ascorbic acid, 2 g acetonitrile, 2 MPa O_2, 80 °C, 12 h.

3. Experimental

3.1. Materials

Aniline, acetonitrile, 1,4-dioxane, ammonium persulfate (98.0%) and ascorbic acid were commercially available. Vanadyl (IV) acetylacetonate (99%) was obtained from Acros Organics (China). The above reagents were used as purchased without further purification unless other noted.

3.2. Catalyst preparation

Briefly, 1000 mg aniline monomer and 265.2 mg $VO(acac)_2$ were dissolved in 20 mL 1.0 M HCl successively. After stirring for 10 minutes, 5 mL 1.0 M HCl solution containing 2.5 g ammonium peroxydisulfate (APS) was added dropwise with vigorous stirring. The polymerization was conducted in an ice bath ($<5\ ^oC$) for 24 h. After evaporation of water at 100 ^oC, the obtained dark-green PANI-V composites were then pyrolyzed under flowing nitrogen at different temperature for 2 h. After calcination, the dark sample was further cooled under nitrogen until to the room temperature. The obtained catalysts were designated as V-N-C.

For comparison, N-C-*600* catalyst was also prepared as the above process but without addition of $VO(acac)_2$.

After the reaction, the reaction mixture was centrifuged and the solid catalysts were recovered, following by washing with ethanol at least three times. The obtained recycled catalysts were calcined under flowing nitrogen at 400^{o}C for 2 hours, and then reused in the next run.

3.3. Catalyst activity test

The hydroxylation of benzene was performed in a Teflon-lined stainless-steel reactor (40 mL) that was equipped with a pressure gauge, thermocouple, gas-inlet valve, magnetic stirrer, and an electric heater with a controller. In a typical experiment, 175 mg of the catalyst, 0.88 g of ascorbic acid, and 10 mmol of benzene were added to 2.0 g of acetonitrile successively. After the system was charged with 2.0 MPa of O_2 at room temperature, the hydroxylation reaction was conducted at 80 ^oC for the desired time under vigorous stirring. After the reaction, 1,4-dioxane was added into the product mixture as an internal standard for product analysis. The mixture was analyzed using a gas chromatograph (GC) of Agilent 7890 equipped with a flame ionization detector (FID). The products of phenol and hydroquinone were detected using GC in this reaction system. The yield of phenol was calculated as: (mole of formed phenol) / (mole of initial benzene) $\times 100$ %.

3.4. Catalyst characterization

Thermogravimetric analysis (TGA) and the corresponding differential thermogravitry (DTG) of the samples were conducted by using a Perkin-Elmer TGA-2 thermo gravimetric analyzer in N_2 from room temperature to 800 ^oC at a rate of 10 ^oC/min. The V loadings of the catalysts were measured by inductively coupled plasma atomic emission spectroscopy (ICP-AES) using a Perkin-Elmer OPTIMA 3300DV. The detection limit was 0.10 ppm. N_2 adsorption-desorption isotherms were determined at -196 °C using a QuadraSorb SI4 Station. Before measurement, the samples were degassed in vacuum at 300 °C for 3 h, and the BET surface areas of the samples were calculated using adsorption data. The crystal structure of V-N-C were characterized with power X-ray diffraction (XRD) patterns on a Rigaku D/Max 2500PC diffractometer equipped with a Cu Ka radiation source (λ = 1.5418 Å) at a scanning rate of 0.05 °/s (2θ from 20 ° to 75 °). Visible Ramman spectra were recorded at room temperature on a Jobin Yvon LabRAM HR 800 instrument with a 532 nm excitation laser at a power of around 20 mW. Surface composition was determined by X-ray photoelectron spectroscopy (XPS) using Thermo Scientific ESCALAB 250Xi instrument with Al-Ka radiation anode ($h\nu$ = 1486.6 eV). The sample was pressed into a sample holder, evacuated in a load lock to 10^{-8} Pa, and transferred to the analysis chamber. The C 1s line (284.6 eV) was used as the reference to correct the banding energies (BE). Scanning electron microscope (SEM) image was conducted On a JSM-7800F microscope operated at 20 kV landing energy.

Conclusion

A series of vanadium-supported N-doped carbon materials (V-N-C) had been synthesized by using polyaniline as the precursor through a facile one-pot pyrolysis method. These catalysts were active for catalyzing the hydroxylation of benzene with molecular oxygen as the oxidant under mild conditions. Especially, V-N-C-*600* catalyst with the higher ratio of V^{4+} was more effective among these catalysts. The reaction time, reaction temperature and oxygen pressure had significant effects on the yield of phenol. A phenol yield of up to 12.6% could be obtained with a selectivity of 97.8%. The V-N-C-*600* catalyst was also stable and could be recycled at least six times without significant decline in yield.

Acknowledgements

The authors thank the financial support from the National Natural Science Foundation of China (Grant No. 21273225).

Notes and references

[a] Dalian Institute of Chemical Physics, Chinese Academy of Sciences, Dalian National Laboratory for Clean Energy, DNL, Dalian, 116023, People's Republic of China. E-mail: sgao@dicp.ac.cn; Fax: +086-0411-84379728; Tel: +086-0411-84379728.

[b] University of Chinese Academy of Sciences, Beijing, 10049, People's Republic of China.

* Corresponding Author: Tel: 086-0411-84379728. Fax: 086-0411-84379728. E-mail: sgao@dicp.ac.cn.

Electronic Supplementary Information (ESI) available: [details of any supplementary information available should be included here]. See DOI: 10.1039/b000000x/

1. J. H. Tyman, *Synthetic and natural phenols*, Elsevier, 1996.
2. M. Weber, M. Weber and M. Kleine‐Boymann, *Ullmann's Encyclopedia of Industrial Chemistry*, 2004.
3. T. Jiang, W. Wang and B. Han, *New J. Chem.*, 2013, **37**, 1654-1664.
4. K. Weissermehl and H. Arpe, VCH, Weinheim, 1988.
5. B. Cornils and W. A. Herrmann, *J. Catal.*, 2003, **216**, 23-31.
6. J. L. Smith and R. Norman, *J. Chem. Soc.*, 1963, 2897-2905.
7. N. Herron and C. A. Tolman, *J. Am. Chem. Soc.*, 1987, **109**, 2837-2839.
8. Y. Liu, K. Murata and M. Inaba, *J. Mol. Catal. A: Chem.*, 2006, **256**, 247-255.
9. Z. Long, Y. Zhou, G. Chen, W. Ge and J. Wang, *Sci. Rep.*, 2014, **4**, 3651.
10. S. Shang, H. Yang, J. Li, B. Chen, Y. Lv and S. Gao, *ChemPlusChem*, 2014, **79**, 680-683.
11. C. Walling and R. A. Johnson, *J. Am. Chem. Soc.*, 1975, **97**, 363-367.
12. H. Mimoun, L. Saussine, E. Daire, M. Postel, J. Fischer and R. Weiss, *J. Am. Chem. Soc.*, 1983, **105**, 3101-3110.
13. M. L. Neidig and K. F. Hirsekorn, *Catal. Commun.*, 2011, **12**, 480-484.
14. P. Borah, X. Ma, K. T. Nguyen and Y. Zhao, *Angew. Chem. Int. Ed.*, 2012, **51**, 7756-7761.
15. P. Zhao, J. Wang, G. Chen, Y. Zhou and J. Huang, *Catal. Sci. Technol.*, 2013, **3**, 1394-1404.
16. G. Ding, W. Wang, T. Jiang, B. Han, H. Fan and G. Yang, *ChemCatChem*, 2013, **5**, 192-200.
17. J.-H. Yang, G. Sun, Y. Gao, H. Zhao, P. Tang, J. Tan, A.-H. Lu and D. Ma, *Energy Environ. Sci.*, 2013, **6**, 793-798.
18. J. Xu, Q. Jiang, T. Chen, F. Wu and Y.-X. Li, *Catal. Sci. Technol.*, 2015, 447-454.
19. M. Iwamoto, J. Hirata, K. Matsukami and S. Kagawa, *J. Phys. Chem.*, 1983, **87**, 903-905.
20. V. Sobolev, A. Kharitonov, Y. A. Paukshtis and G. Panov, *J. Mol. Catal.*, 1993, **84**, 117-124.
21. R. Leanza, I. Rossetti, I. Mazzola and L. Forni, *Appl. Catal., A*, 2001, **205**, 93-99.
22. J. Jia, K. S. Pillai and W. M. Sachtler, *J. Catal.*, 2004, **221**, 119-126.
23. V. S. Chernyavsky, L. V. Pirutko, A. K. Uriarte, A. S. Kharitonov and G. I. Panov, *J. Catal.*, 2007, **245**, 466-469.
24. S.-i. Niwa, M. Eswaramoorthy, J. Nair, A. Raj, N. Itoh, H. Shoji, T. Namba and F. Mizukami, *Science*, 2002, **295**, 105-107.
25. K. LunáYeung, *Chem. Commun.*, 2009, 5898-5900.
26. X. Wang, X. Tan, B. Meng, X. Zhang, Q. Liang, H. Pan and S. Liu, *Catal. Sci. Technol.*, 2013, **3**, 2380-2391.
27. T. Ohtani, S. Nishiyama, S. Tsuruya and M. Masai, *J. Catal.*, 1995, **155**, 158-162.
28. J. Okamura, S. Nishiyama, S. Tsuruya and M. Masai, *J. Mol. Catal. A: Chem.*, 1998, **135**, 133-142.
29. T. Miyahara, H. Kanzaki, R. Hamada, S. Kuroiwa, S. Nishiyama and S. Tsuruya, *J. Mol. Catal. A: Chem.*, 2001, **176**, 141-150.
30. X. Gao and J. Xu, *Catal. Lett.*, 2006, **111**, 203-205.
31. S. Sumimoto, C. Tanaka, S.-t. Yamaguchi, Y. Ichihashi, S. Nishiyama and S. Tsuruya, *Ind. Eng. Chem. Res.*, 2006, **45**, 7444-7450.
32. H. Ge, Y. Leng, C. Zhou and J. Wang, *Catal. Lett.*, 2008, **124**, 324-329.
33. H. Yang, J.-Q. Chen, J. Li, Y. Lv and S. Gao, *Applied Catalysis A, General*, 2012, **415**, 22-28.
34. H. Yang, J. Li, L. Wang, W. Dai, Y. Lv and S. Gao, *Catal. Commun.*, 2013, **35**, 101-104.
35. Y.-Y. Gu, X.-H. Zhao, G.-R. Zhang, H.-M. Ding and Y.-K. Shan, *Appl. Catal., A*, 2007, **328**, 150-155.
36. W. Wang, G. Ding, T. Jiang, P. Zhang, T. Wu and B. Han, *Green Chem.*, 2013, **15**, 1150-1154.
37. K. Gong, F. Du, Z. Xia, M. Durstock and L. Dai, *Science*, 2009, **323**, 760-764.
38. R. Nie, J. Shi, W. Du, W. Ning, Z. Hou and F.-S. Xiao, *J. Mater. Chem. A*, 2013, **1**, 9037-9045.
39. G. Wu, K. L. More, C. M. Johnston and P. Zelenay, *Science*, 2011, **332**, 443-447.
40. M. Baibarac, I. Baltog, S. Lefrant, J. Mevellec and O. Chauvet, *Chem. Mater.*, 2003, **15**, 4149-4156.
41. S. B. Kristensen, A. J. Kunov-Kruse, A. Riisager, S. B. Rasmussen and R. Fehrmann, *J. Catal.*, 2011, **284**, 60-67.
42. N. Pinna, M. Willinger, K. Weiss, J. Urban and R. Schlögl, *Nano Lett.*, 2003, **3**, 1131-1134.
43. L. Lin, Q. Zhu and A.-W. Xu, *J. Am. Chem. Soc.*, 2014, **136**, 11027-11033.
44. A. Sadezky, H. Muckenhuber, H. Grothe, R. Niessner and U. Pöschl, *Carbon*, 2005, **43**, 1731-1742.
45. Y. Nabae, S. Moriya, K. Matsubayashi, S. M. Lyth, M. Malon, L. Wu, N. M. Islam, Y. Koshigoe, S. Kuroki and M.-a. Kakimoto, *Carbon*, 2010, **48**, 2613-2624.
46. U. Koslowski, I. Herrmann, P. Bogdanoff, C. Barkschat, S. Fiechter, N. Iwata, H. Takahashi and H. Nishikori, *ECS Trans.*, 2008, **13**, 125-141.
47. G. Wu, C. M. Johnston, N. H. Mack, K. Artyushkova, M. Ferrandon, M. Nelson, J. S. Lezama-Pacheco, S. D. Conradson, K. L. More and D. J. Myers, *J. Mater. Chem.*, 2011, **21**, 11392-11405.
48. Y. Zhao, K. Watanabe and K. Hashimoto, *J. Am. Chem. Soc.*, 2012, **134**, 19528-19531.
49. S. Kundu, T. C. Nagaiah, W. Xia, Y. Wang, S. V. Dommele, J. H. Bitter, M. Santa, G. Grundmeier, M. Bron and W. Schuhmann, *J. Phys. Chem. C*, 2009, **113**, 14302-14310.
50. H. Peng, Z. Mo, S. Liao, H. Liang, L. Yang, F. Luo, H. Song, Y. Zhong and B. Zhang, *Sci. Rep.*, 2013, **3**, 1765.
51. T. Sharifi, G. Hu, X. Jia and T. Wågberg, *ACS nano*, 2012, **6**, 8904-8912.
52. J. Xu, H. Liu, R. Yang, G. Li and C. Hu, *Chin. J. Catal.*, 2012, **33**, 1622-1630.
53. Y. He, Y. Wang, L. Zhao and X. Wu, *J. Mol. Catal. A: Chem.*, 2011, **337**, 61-67.
54. Y.-k. Masumoto, R. Hamada, K. Yokota, S. Nishiyama and S. Tsuruya, *J. Mol. Catal. A: Chem.*, 2002, **184**, 215-222.
55. S.-t. Yamaguchi, S. Sumimoto, Y. Ichihashi, S. Nishiyama and S. Tsuruya, *Ind. Eng. Chem. Res.*, 2005, **44**, 1-7.